YANQIU ZHAO[1], SHUANG WANG[2], YONGCUN GUO[3], GANG CHENG[4],
LEI HE[5], WENSHAN WANG[6]

The identification of coal and gangue and the prediction of the degree of coal metamorphism based on the EDXRD principle and the PSO-SVM model

Introduction

Nowadays, coal is the world's main energy source and raw coal needs to be washed and processed after mining in order to be used. The separation of coal from gangue is an essential part of the coal production process, as gangue is an inevitable waste product of the coal

✉ Corresponding Author: Yanqiu Zhao; e-mail: yqzhao0912@163.com

[1] School of Mechanical Engineering, Anhui University of Science and Technology, China; ORCID iD: 0000-0001-5171-3367; e-mail: yqzhao0912@163.com
[2] School of Mechanical Engineering, Anhui University of Science and Technology, China; e-mail: shuangw094@126.com
[3] School of Mechanical Engineering, Anhui University of Science and Technology, China; e-mail: guoyc@aust.edu.cn
[4] School of Mechanical Engineering, Anhui University of Science and Technology, China; e-mail: gang740@126.com
[5] School of Mechanical Engineering, Anhui University of Science and Technology, China; e-mail: helei_jxzl@126.com
[6] School of Mechanical Engineering, Anhui University of Science and Technology, China; e-mail: wwsaust@126.com

mining process. Waste rock removal is the basis for the production of clean energy from coal, and the reduction of waste rock particle can reduce PM2.5 emissions (Cao et al. 2020; Alfarzaeai et al. 2020). Continuous attention is paid to the quality of coal and environmental protection nowadays; with conventional coal and gangue sorting technologies, there exists a large labor force, non-automation, water waste and pollution of the environment and other shortcomings which cannot meet the development of green mines and coal mine intelligence (Sun et al. 2019). New coal and gangue sorting technology has rapidly appeared and fruitful results have been achieved.

Dry ray coal-separation technology has entered a rapid development stage since the 21st century with the development of dual-energy X-ray based coal and gangue separation devices by RWTH Aachen University in Germany, the University of Witwatersrand in South Africa, and the Federal University of Rio de Janeiro in Brazil on their own or in cooperation with companies (Robben et al. 2019; Von Ketelhodt et al. 2010). Research on X-ray coal and gangue separation has been carried out by a number of universities since 2010, focusing on the identification of coal and gangue as well as the optimization of the separation system and the extraction of X-ray image recognition features in conjunction with the improvement of the recognition algorithm (Kuerten 2017; Wang 2021). In 2015, the successful application of the Deep Face project in face recognition and the emergence of Alpha Go Zero proved that deep learning algorithms are a cut above the rest in image recognition (Ranjan et al. 2017; Silver et al. 2016). This technique has also been applied to coal and gangue image detection by researchers, mainly from coal and gangue image feature fusion (Singh et al. 2006), network light-weighting (Xu et al. 2020), and light source type transformation (Zhang et al. 2022). Nonetheless, the application of coal and gangue identification methods based on machine vision is severely restricted by a series of objective conditions such as downhole dust, noise, light and space. The rapid development of spectral technology and sensor technology in recent years has set off a boom in the infrared spectral identification of coal and gangue. Song et al. (Song et al. 2017) found that coal and gangue had "different bodies with the same spectrum" in the visible-near-infrared band and proposed a coal and gangue classification method based on visible-near-infrared and thermal infrared spectral conjoint analysis. Achievements of the above experimental research for the solution of coal and gangue identification are of guiding significance. As a result of these studies, the identification of coal and gangue has been studied, but the refined identification of coal types has been neglected.

Stored in China from lignite with a low degree of metamorphism to anthracite with a high degree of metamorphism, characterizing the degree of metamorphism, whereby the coal tends to approach graphite, is the basis for an in-depth study of coal refinement identification. According to the degree of metamorphism, coals are mainly divided into the following three types: low-deteriorated coal, such as, lignite, long-flame coal and gas coal, the vitrinite of which means random reflectance (Rran) is less than 0.6%; medium-deteriorated coal, such as, gas-fat coal, fat coal, coking coal, for which Rran is 0.6~2.0%; high-deteriorated coal, such as lean coal, poor coal, anthracite coal, with Rran larger than 2.0% (Energy/2000/12). Methods for characterizing the metamorphism degree of coal currently includes optical

microscopy, microscope photometer, electron microscopy, Raman and infrared spectroscopy, and X-ray analysis (Bassett et al. 2006; Xin et al. 2014). Of these strategies, the X-ray diffraction method is a more ideal method to determine the metamorphism degree of coal as the information obtained directly reflects the microstructural information of coal in comparison with several other methods (Wang et al. 1998; Saikia et al. 2008). Ju et al and Xiang et al. (Ju et al. 2014; Xiang et al. 2016) studied the microcrystalline structure in coal and the carbon structure characteristics of coals with different degrees of metamorphism using XRD. The more consistent view was that as the metamorphism degree of coal increased, the aliphatic structure in coal decreased and the aromatic structure increased, and the structure of coal gradually tended to be graphitized (Luo et al. 2004; Barnakov et al. 2016). Based on this conclusion, Qian et al. (Qian et al. 2017) used XRD to analyze the layer spacing (d_{002}) and stacking height (L_{002}) of the aromatic structural units of coal dust, and then determined the degree to which the crystal structure converged to graphite before and after the coal dust explosion by the changes in d_{002} and L_{002}. The above studies, known as the ADXRD technique, have investigated the degree of coal deterioration, but the ADXRD technique is unable to meet the real-time requirements of item detection. With advantages such as simple system structure, no need for angular scanning structure and high work efficiency compared to ADXRD, the EDXRD technique is widely used for the real-time detection of items (Luggar et al. 1998). A proposal was made by Tongji University in 2019 to apply "energy dispersive X-ray diffraction" to the field of security inspection to achieve the accurate investigation of luggage and courier boxes (Chen et al. 2019). Nevertheless, applications of EDXRD technology in the field of coal and gangue identification have rarely been reported.

By combining the advantages of the ADXRD technique in characterizing the metamorphism degree of coal and the real-time nature of the EDXRD technique in detecting the items, this paper investigates coal and gangue identification and the prediction of the coal metamorphism degree based on the X-ray diffraction principle. Major coal varieties as well as gangue in the Huainan mining area were studied in this paper and both ADXRD and EDXRD patterns of the samples were collected. Differences in the physical phase information contained in the EDXRD patterns of coal and gangue are analyzed to extract the identification features of coal and gangue and to achieve the identification of coal and gangue by the PSO-SVM model. Then, the ADXRD technique for characterizing the metamorphism degree of coal was converted into the EDXRD technique, which was embedded in the PSO-SVM identification model to achieve the model's prediction of the metamorphism degree of coal for the purpose of the initial screening of coal types.

1. Materials

The coal used in this study was all mined from the main mining seam 11[#] of the Pan San Mine in the Huainan Coal field, and the detailed parameters are shown in Table 1. The instruments used for the proximate analysis, the vitrinite mean random reflectance and the

Table 1.   The detailed parameters of samples

Tabela 1.   Szczegółowe parametry próbek

Number of coal seam	Name of working surface	Mining depth (m)	Coal type
11–2	1 231(1)	–625 ~ 759	1/3 coking coal
	2 121(1)	–780 ~ –818	gas coal

Table 2.   Proximate analysis and elemental analysis of the coal samples

Tabela 2.   Analiza bezpośrednia i analiza elementarna próbek węgla

Coal type	Proximate analysis (wt%)					Vitrinite Mean Random Reflectance
	Mad	Aad	Vadf	Vad	FCad	Rran (%)
1/3 coking coal	0.8	19.2	34.8	27.8	52.2	0.61
Gas coal	1.0	40.0	38.9	22.9	36.1	0.54
Coal type	Elemental analysis (wt%)				
	Cad	Had	Oad	Nad	St, ad
1/3 coking coal	57.3	2.6	18.7	0.5	0.2
Gas coal	54.0	3.9	9.9	0.7	0.4

elemental analysis of the coal samples were SX2-10-12N, HD Microphotometer and Elementar Vario EL III, respectively, and the results are as shown in Table 2.

The suffix "ad" means that when the coal quality is analyzed, the coal is in a state of air drying.

Proximate analysis:
- Mad: moisture in coal when it is dry in the air.
- Aad: ash content, is the remains of minerals in coal that have been burned and decomposed under air drying.
- Vad: volatile, is calculated from the dry matter of coal (excluding water), and the calculation formula is shown in Equation (1).

$$Vad = \frac{m_1}{m} \cdot 100 - Mad \tag{1}$$

Where m is the quality of test samples, and its unit is grams; m_1 is the reduced mass of coal after heating, and its unit is grams.

Vdaf: volatiles without ash, this is the volatile calculated after deducting moisture and ash. The calculation formula is shown in Equation (2).

$$Vdaf = \frac{Vad}{100 - Mad - Aad} \cdot 100 \tag{2}$$

◆ FCad: Fixed carbon in coal. The calculation formula is shown in Equation (3).

$$FCad = 100 - (Mad + Aad + Vad) \tag{3}$$

Elemental analysis:
◆ Cad: represents the carbon content of the coal.
◆ Had: represents the hydrogen content of the coal.
◆ Oad: represents the oxygen content of the coal.
◆ Nad: represents the nitrogen content of the coal.
◆ St,ad: total sulfur, represents the total sulfur content of coal, including organic sulfur and inorganic sulfur.

2. Experimental principles and methods

2.1. EDXRD pattern acquisition

The test was supported by Shanghai Microspectrum Chemical Technology Service Co., Ltd. Figure 1 shows the working principle of EDXRD, the X-ray is generated by an X-ray tube, which penetrates the sample and then diffracts. The diffracted X-ray enters the detector, which is processed by the data analyzer to obtain the EDXRD pattern. The operating angle θ is fixed, and the formula of the EDXRD principle can be expressed as (Cook et al. 2007):

$$E = \frac{hc}{2d \sin\left(\dfrac{\theta}{2}\right)} \tag{4}$$

E is the X-ray energy, h and c are Planck's constant and lightspeed, respectively, d is the interplanar spacing, and θ is the operating angle.
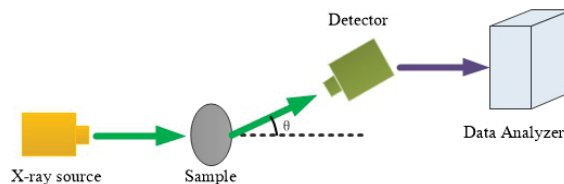

Fig. 1. Schematic diagram of the EDXRD

Rys. 1. Schemat ideowy EDXRD

A tungsten target X-ray tube was used to generate the X-ray energy spectrum with an operating voltage and current of 80 kV and 10 mA, respectively, and the detector was a CdTe energy spectrum detector with a crystal area of 25 mm^2 and an energy resolution of 0.6 keV at 60 KeV. The operating angle was 5° and the energy resolution of the system was $\Delta E/E = 0.0355$.

2.2. ADXRD pattern acquisition

The Smartlab SE X-ray diffractometer from Rigaku Corporation was used for this test to analyze the phase composition of the samples. Figure 2 shows the working principle of ADXRD – X-rays with single energy irradiate the object that is to be measured. The detector scans around the object at a certain angular velocity, and when the angle satisfies Bragg's diffraction law, as shown in Equation 5, an ADXRD pattern about the diffraction angle and the intensity of the diffracted light is obtained (Zhu et al. 1987).

$$2d \sin \theta = n\lambda \qquad (5)$$

✎ θ – angle between an incoming ray and a reflected crystal surface,
  d – interplanar distance,
  n – diffraction order,
  λ – wavelength of X-ray.

The anode target is Cu Kα target, the X-ray tube voltage is 40 kV, the working current is 150 mA, the scanning speed is 10°/min, and the scanning range (2θ) is 20°~55°.
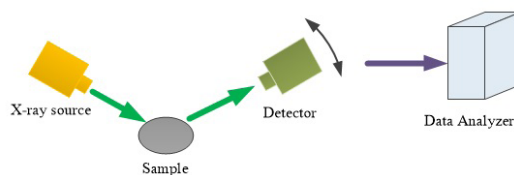

Fig. 2. Schematic diagram of the ADXRD

Rys. 2. Schemat ideowy ADXRD

2.3. PSO-SVM Recognition model

Classification or regression prediction models generally adopt SVM, neural networks, decision trees, clustering, and other modeling methods in the case of small data sets (Wang et al. 2021), of which SVM has a better classification effect. In this paper, the Libsvm-Faruto

Ultimate software package was adopted to achieve coal and gangue classification, which can solve multi-classification problems, regression problems, and distribution estimation problems (Zhang et al. 2020). Libsvm-Faruto Ultimate, written by Faruto and Li yang, is a toolbox with implementations for support vector machines based on libsvm (Chang et al. 2011). For the SVM model, choosing a suitable kernel is imperative to the success of the learning process. Since the Gaussian radial basis function has a strong ability to deal with different characteristic parameters and nonlinear class relations (Guo et al. 2021), the gaussian radial basis function is adopted as the kernel function in this paper. The hyperplane discriminant function and kernel function of SVM classification established in this paper are expressed as follows:

$$f(x) = \text{sgn}\left[\sum_{i \in SV} y_i a_i K(x, x_i) + b \right] \tag{6}$$

$$K(x, x_i) = \exp\left(-\frac{\|x - x_i\|^2}{2g^2} \right) \tag{7}$$

↳ sgn –   symbolic function,
   SV –   set of support vector points,
   $K(xi, x)$ –   kernel function,
   g –   width of the Gaussian meridional basis kernel function.

Compared with Libsvm, Libsvm-Faruto adds more functions, such as grid search, genetic algorithm (GA) and particle swarm optimization (PSO) algorithms to optimize the penalty
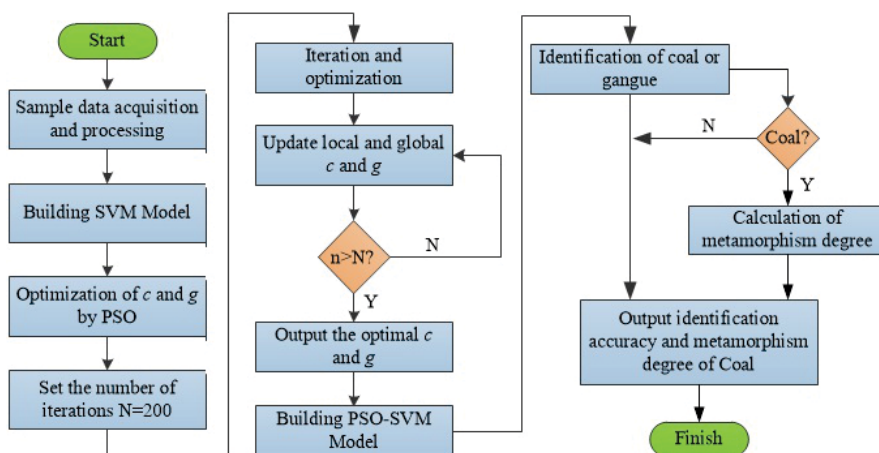

Fig. 3. The specific algorithm flow of PSO-SVM

Rys. 3. Specyficzny przebieg algorytmu PSO-SVM

parameter (*c*) and kernel function parameter (*g*). The particle swarm optimization (PSO) algorithm is a global optimization algorithm for evolutionary computation techniques, which has advantages in terms of parameter selection and convergence speed (Shrivastava et al. 2015). The PSO algorithm is used in the paper to seek the optimal combination of parameters c and g. The specific algorithm flow is shown in Figure 3.

3. Results and discussion

3.1. ADXRD and EDXRD pattern analysis of gas coal, 1/3 coking coal and gangue

Figure 4 shows the ADXRD and EDXRD patterns of gangue, gas coal and 1/3 coking coal. Gangue (as shown in Figure 4a) shows distinctive peaks around A = 21, 27 and 50°, corresponding to 100, 101 and 112 diffraction peaks of SiO_2, respectively. A = 25° is the diffraction peak of kaolinite, indicating that the physical phase of the gangue is mainly SiO_2 with a small amount of kaolinite. The diffraction peaks at around A = 25° of gas coal and 1/3 coking coal (shown in Figures 4b and c) correspond to the 002 diffraction peak of graphite which reflects the degree of parallel orientation of the aromatic structural units in coal, namely, the vertical order degree of aromatic structural units (Xiang et al. 2016).

As Figure 5 shows, gangue has obvious diffraction peaks at around E = 35 KeV and 44 KeV (Figure 5a), gas coal has obvious diffraction peaks at around E = 40 KeV and 43 KeV (Figure 5b), and 1/3 coking coal has broad diffraction peaks at around E = 40 KeV
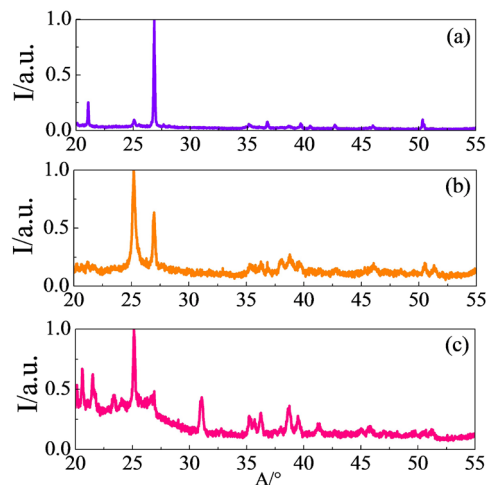

Fig. 4. The ADXRD patterns of gangue (a), gas coal (b) and 1/3 coking coal (c)

Rys. 4. Modele ADXRD skały płonnej (a), węgla gazowego (b) i 1/3 węgla koksowego (c)

(Figure 5c). Based on equations (4) and (5), the interplanar spacing d corresponding to the positions of diffraction peaks in the EDXRD and ADXRD patterns of gangue, gas coal, and 1/3 coking coal can be calculated, the results of which are shown in Table 3. As can be seen from Table 3, in the EDXRD pattern of gas coal, the diffraction peaks at E ≈ 40 KeV and
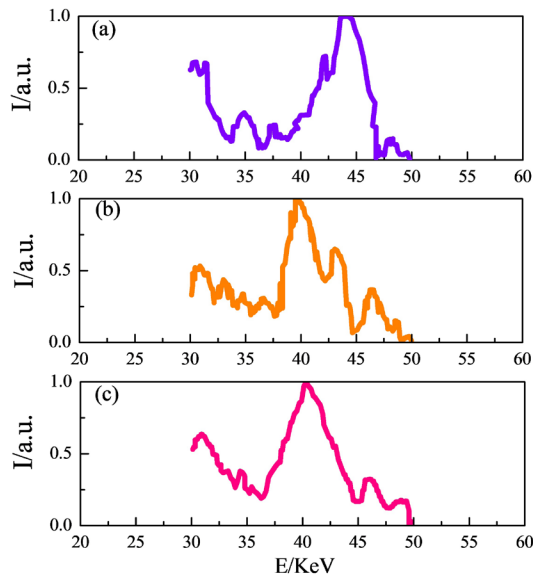

Fig. 5. The EDXRD patterns of gangue (a), gas coal (b) and 1/3 coking coal (c)

Rys. 5. Wzorce EDXRD skały płonnej (a), węgla gazowego (b) i 1/3 węgla koksowego (c)

Table 3.   The Position diffraction peaks and corresponding plane spacing d in EDXRD and ADXRD patterns of gangue, gas coal and 1/3 coking coal

Tabela 3.   Piki dyfrakcji położenia i odpowiadające im odstępy między płaszczyznami d we wzorcach EDXRD i ADXRD skały płonnej, węgla gazowego i 1/3 węgla koksowego

Item	EDXRD		ADXRD	
	diffraction peak Position (KeV)	d (nm)	diffraction peak Position (°)	d (nm)
Gangue	34.6	0.40	21.0	0.42
	44.0	0.32	26.8	0.33
Gas coal	40.3	0.35	25.2	0.35
	42.8	0.33	26.9	0.33
1/3 Coking coal	40.0	0.35	25.1	0.35

43 KeV correspond to the interplanar spacing d values of 0.35 nm and 0.33 nm, respectively, in the ADXRD pattern of gas coal, the diffraction peaks at around A = 21° and 27° corresponds to the interplanar spacing d values of 0.35 nm and 0.33 nm, according to the results of gas coal's ADXRD pattern, the diffraction peaks of gas coal at E ≈ 40 KeV and 43 KeV represent the (002) crystal plane of graphite and (101) crystal plane of SiO_2, respectively. Similarly, in the EDXRD pattern of gangue, the diffraction peaks at E ≈ 35 KeV and 44 KeV correspond to the (100) and (101) crystal planes of quartz, respectively. In the EDXRD pattern of 1/3 coking coal, the diffraction peak at E ≈ 40 KeV represents the (002) crystal plane of graphite.

3.2. Prediction of the degree of coal metamorphism

Coal is not crystalline, but a fraction of ordered carbon is present within it, and this is formed by stacking several aromatic structural units in the coal at different degrees of parallelism, called microcrystals. Analysis by X-ray diffraction can reveal the orderliness of the arrangement of carbon atoms in coal (Jiang et al. 1998; Saikia 2010) leading to an analysis of the metamorphism degree of coal.

The degree of metamorphism of coal, which can be expressed by the degree of graphitization, was proposed by two scientists, Mering and Marie, in conjunction with Franklin's carbon structure model, and can be expressed in a simplified form as:

$$G = (0.3340 - d_{002})/(0.3340 - 0.3354) \qquad (8)$$

✎ G – the graphitization degree of coal-series cryptocrystalline graphite,
   0.3340 – the carbon interlayer spacing of a disordered structure,
   0.3354 – the interlayer spacing of complete graphitized carbon,
   $d_{(002)}$ – the interplanar spacing corresponding to the (002) diffraction peak
                  of the graphite in the ADXRD pattern.

According to Section 4.1, the ADXRD pattern of 1/3 coking coal and gas coal shows that the diffraction peak at around A = 25° represents the (002) crystal plane and $d_{(002)}$ can be calculated according to Equation (5). In the EDXRD patterns of 1/3 coking coal and gas coal, the diffraction peak at around E = 40 KeV represents the (002) crystal plane and $d_{(002)}$ can be calculated according to Equation (4). The graphitization values of 1/3 coking coal and gas coal in Figure 4 and 5 calculated by the ADXRD technique and the EDXRD technique are shown in Table 4. A graphitization error of no more than 5% can be seen from Table 4 for both techniques; therefore, the EDXRD technique predicts the graphitization of coal with improved efficiency and no loss of accuracy.

Table 4.   The graphitization degree of 1/3 coking coal and gas coal calculated *b* ADXRD and EDXRD

Tabela 4.   Obliczony stopień grafityzacji 1/3 węgla koksowego i gazowego *b* ADXRD i EDXRD

ADXRD Item	A (°)	d(002) (nm)	G (%)
1/3 Coking coal	25.12	0.3545	14.64
Gas coal	25.2	0.3534	13.86
EDXRD Item	E/KeV	d(002) (nm)	G (%)
1/3 Coking coal	39.97	0.3558	15.57
Gas coal	40.33	0.3527	13.36

3.3. Identification of coal and gangue and the prediction of the metamorphism degree of coal based on the EDXRD principle

In this investigation, 122 EDXRD patterns were used as data sets for the coal and gangue identification model, including thirty pieces of 1/3 coking coal, thirty-two pieces of gas coal and sixty pieces of gangue. As can be seen from Section 4.1, the difference of EDXRD patterns of samples is mainly affected by phase type. Therefore, The EDXRD pattern-recognition features are extracted mainly for the main diffraction peaks representing the phase of the samples. The identification characteristics of some samples are shown in Figure 6 and given a label of 1 for 1/3 of coking coal and gas coal and 2 for gangue. Figure 6a, b and c are the identification characteristics of gangue, gas coal and 1/3 coking coal, respectively.
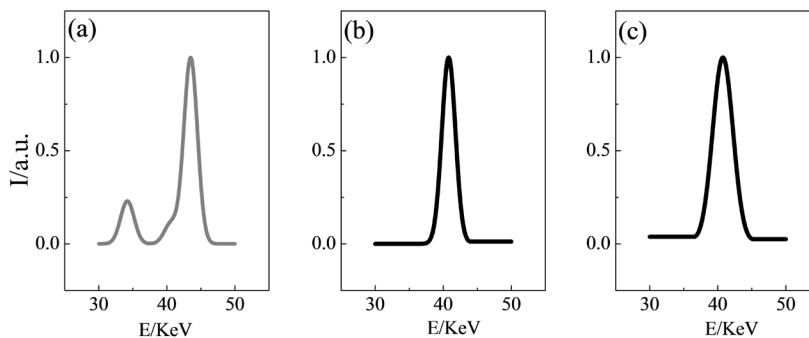

Fig. 6. The identification characteristics of gangue (a), gas coal (b), 1/3 coking coal (c)

Rys. 6. Charakterystyki identyfikacyjne skały płonnej (a), węgla gazowego (b), węgla koksowego 1/3 (c)

The diffraction peak of coal (E ≈ 40 KeV) represents (002) crystal plane, and the diffraction peak of gangue (E ≈ 35 KeV, 44 KeV) represents (100) crystal plane and (101) represents crystal plane of quartz.

The data set was randomly sorted, and the training set and test set were divided at a ratio of 2:1. The PSO-SVM recognition model was established in accordance with Section 3.3. The optimal hyper-parameter combination of the recognition model was c = –100 and g = –0.01. The recognition accuracy of the training set and the test set were 100% and 97.56%, respectively. Figure 7 shows the actual classification and predicted classification for the test set, as can be seen from which, the recognition accuracy of this model for gangue is 100%, and there is a misrecognition for coal. The metamorphism degree of the coal in the PSO-SVM model output test set is shown in Table 5. A rough prediction of the coal type
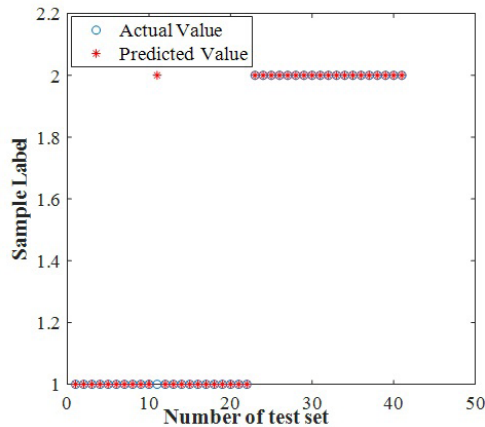

Fig. 7. Actual and predicted classification for test set

Rys. 7. Aktualna i przewidywana klasyfikacja zbioru testowego

Table 5.   The metamorphism degree of coal in test set

Tabela 5.   Stopień metamorfizmu węgla w zestawie testowym

Sample No.	G (%)	Sample No.	G (%)	Sample No.	G (%)
1	12.93	8	10.57	15	8.07
2	7.86	9	8.14	16	8.36
3	11.21	10	12.36	17	11.07
4	12.71	11	6.36	15	7.79
5	11.07	12	7.50	19	10.07
6	13.00	13	10.57	20	10.43
7	13.29	14	11.07	21	9.93

can be made based on the degree of metamorphism G. As the maximum value of G is 13%, a rough estimate of the degree of metamorphic weakness of the coal as a whole can be made, which is consistent with the industrial analysis results of coal samples in Section 2.

3.4. Experimental validation

Sixty EDXRD patterns of coal and gangue were randomly collected and the diffraction peaks of the main phases were extracted as identification features using PSO-SVM as the classification model and the final classification results were experimentally observed as shown in Table 6. Following experimental verification, the accuracy of coal and gangue identification based on the X-ray diffraction principle was 96.66%; furthermore, the metamorphism of coal was predicted while the target was identified, as shown in Table 7.

Table 6.   Recognition Results of Validation Set

Tabela 6.   Wyniki rozpoznawania zestawu walidacyjnego

Recognition model	Number of validation set	Recognition accuracy	Misidentification/ /coal	Misidentification/ /gangue
PSO-SVM	60	96.66%	2/30	0/30

Tabel 7.   The degree of metamorphism of coal in the validation set

Tabela 7.   Stopień metamorfizmu węgla w zbiorze walidacyjnym

Sample No.	G (%)	Sample No.	G (%)	Sample No.	G (%)
1	5.78	11	13.14	21	9.36
2	6.79	12	6.71	22	5.36
3	7.86	13	6.00	23	6.79
4	5.71	14	7.64	24	10.71
5	5.64	15	6.93	25	7.29
6	11.36	16	13.14	26	7.07
7	7.43	17	10.00	27	6.43
8	10.00	18	11.50	28	7.64
9	8.21	19	9.21		
10	8.86	20	5.36		

Conclusions

This paper proposed the identification of coal and gangue as well as the prediction of the degree of coal metamorphism based on the X-ray diffraction theory, and the following conclusions were obtained.

1. The correlation between the ADXRD patterns of 1/3 coking coal, gas coal and gangue and the EDXRD patterns are analyzed in this paper. In the EDXRD pattern of 1/3 coking coal, the diffraction peak at E ≈ 40 KeV corresponded to the diffraction peak at A ≈ 25° in the ADXRD pattern, representing the (002) crystal plane of graphite. In the EDXRD patterns of gas coal, the diffraction peaks at E ≈ 40 KeV and 43 KeV corresponded to the diffraction peaks at A ≈ 25 and 27° in the ADXRD patterns, representing the (002) crystal plane of graphite and (101) crystal plane of quartz, respectively. In the EDXRD pattern of gangue, the diffraction peaks at E ≈ 35 KeV and 44 KeV corresponded to the diffraction peaks at A ≈ 21 and 27° in the ADXRD pattern, representing the (100) and (101) crystal planes of SiO_2, respectively.

2. The error in calculating the graphitization of 1/3 coking coal and gas coal using the ADXRD technique is no more than 5% compared to the EDXRD technique. Therefore, the EDXRD technique predicts the graphitization of coal with increased efficiency and no loss of accuracy.

3. Major diffraction peaks representing the physical phase of the samples were used as identification features of the PSO-SVM model, with 96.66% accuracy of coal and gangue identification in the validation set. The metamorphism degree of coal G output from the PSO-SVM model could roughly estimate the metamorphism degree of weakness of the coal used in this paper, which is consistent with the results of the proximate analysis of coal samples in Section 2.

The results of this paper will lay a technical foundation for optimizing the energy structure and improving the energy-utilization rate, with important theoretical significance and value for engineering applications.

REFERENCES

Alfarzaeai et al.2020 – Alfarzaeai, M., Niu, Q., Zhao, J., Eshaq, R. and Hu, E. 2020. Coal/Gangue Recognition Using Convolutional Neural Networks and Thermal Images. *IEEE Access* 8, pp. 76780–76789.

Barnakov et al. 2016 – Barnakov, C., Khokhlova, G., Popova, A., Sozinov, S. and Ismagilov, Z. 2016. X-Ray diffraction technique: structure determination of carbonaceous materials (Review). *Chemistry for Sustainable Development* 24(4), pp. 569–576.

Bassett et al. 2006 – Bassett, K., Ettmuller, F. and Bemet, M. 2006. Provenance analysis of the Paparoa and Brunner coal measures using integrated SEM-cathodoluminescence and optical microscopy. *New Zealand Journal of Geology and Geophysics* 49(2), pp. 241–254, DOI: 10.1080/00288306.2006.9515163.

Cao et al. 2020 – Cao, Y., Liu, M., Xing, Y., Li, G., Luo, J. and Gui, X. 2020. Current situation and prospect of underground coal preparation technology. *Journal of Mining and Safety Engineering* 37(01), pp. 192–201 (*in Chinese*).

Chang et al. 2011 – Chang, C. and Lin, C. 2011. LIBSVM: a library for support vector machines. *ACM Transactions on Intelligent Systems and Technology* 2(3), pp. 1–27, DOI: 10.1145/1961189.1961199.

Chen et al. 2019 – Chen, Y., Wang, X., Song, Q., Xu, J. and Mu, B. 2019. Development of a high-energy-resolution EDXRD system with a CdTe detector for security inspection. *AIP Advances* 8(10), DOI: 10.1063/1.5052027.

Cook et al. 2007 – Cook, E., Fong, R., Horrocks, J., Wilkinson, D. and Speller, R. 2007. Energy dispersive X-ray diffraction as a means to identify illicit materials: A preliminary optimisation study. *Applied radiation and isotopes* 65, pp. 959–967, DOI: 10.1016/j.apradiso.2007.02.010.

Energy/2000/12 – (E/ECE/)Energy/2000/12, International Codification System for Low-rank Coal Utilization.

Jiang et al. 1998 – Jiang, B., Qin, Y., Song, D. and Wang, C. 1998. XRD structure of high rank tectonic coals and its implication to structural geology. *Journal of China University of mining and Technology* 27(2), pp. 115–118. (*in Chinese*).

Ju et al. 2014 – Ju, Y., Luxbacher, K., Li, X., Wang, G., Yan, Z., Wei, M. and Yu, L. 2014. Micro-structural evolution and their effects on physical properties in different types of tectonically deformed coals. *International Journal of Coal Science and Technology* 1, pp. 364–375. DOI: 10.1007/s40789-014-0042-1.

Kuerten, A. 2017. Coal preconcentration in Moatize mine based on sensor-SBS technology. Rio de Janeiro: Federal University of Rio Grande Do Sul.

Luggar et al. 1998 – Luggar, R., Farquharson, M., Horrocks, J. and Lacey, R. 1998. Multivariate Analysis of Statistically Poor EDXRD Spectra for the Detection of Concealed Explosives. *X-ray Spectrometry* 27, pp. 87–94, DOI: 10.1002/(SICI)1097-4539(199803/04)27:2<87::AID-XRS256>3.0.CO;2-0.

Luo et al. 2004 – Luo, Y. and Li, W. 2004. X- ray diffraction analysis on the different macerals of several low-to-medium metamorpic grade coals. *Journal of China Coal Society* 03, pp. 338–341 (*in Chinese*).

Qian et al. 2017 – Qian, J., Liu, Z., Lin, S., Li, X., Hong, S. and Li, D. 2017. Characteristics analysis of post-explosion coal dust samples by X-ray diffraction. *Combustion Science and Technology* 190(1), pp. 1–15, DOI: 10.1080/00102202.2017.1407317.

Ranjan et al. 2017 – Ranjan, R., Patel, V. and Chellappa, R. 2017. Hyper Face: a deep multi-task learning framework for face detection, landmark localization, pose estimation, and gender recognition. *IEEE Transactions on Pattern Analysis and Machine Intelligence* 41(1), pp. 121–135, DOI: 10.48550/arXiv.1603.01249.

Robben et al. 2019 – Robben, C. and Hermann, W. 2019. Sensor-Based Ore Sorting Technology in Mining-Past, Present and Future. *Minerals* 9(9), pp. 523–426, DOI: 10.3390/min9090523.

Saikia, B. 2010. Inference on carbon atom arrangement in the turbostatic graphene layers in Tikak coal (India) by X-ray pair distribution function analysis. *International Journal of Oil, Gas and Coal Technology* 3(4), pp. 362–372, DOI: 10.1504/IJOGCT.2010.037465.

Saikia et al. 2008 – Saikia, B., and Boruah, R. 2008. Structural studies of some Indian coals by using X-ray diffraction techniques. *Journal of X-Ray Science and Technology* 16(2), pp. 89–94.

Shrivastava et al. 2015 – Shrivastava, N., Khosravi, A. and Panigrahi, B. 2015. Prediction interval estimation of electricity prices using PSO-tuned support vetor machines. *IEEE Transactions on Industrial Informatics* 11(2), pp. 322–331, DOI: 10.1109/TII.2015.2389625.

Silver et al. 2016 – Silver, D., Huang, A., Maddison, C., Guez, A., Sifre, L., Driessche, G., Schittwieser, J., Antonoglou, L., Panneershelvam, V., Lanctot, M., Dieleman, S., Grewe, D., Nham, J., Kalchbrenner, N., Sutskever, I.,

Lillicrap, T., Leach, M., Kavukcuoglu, K., Graepel, T. and Hassabia, D. 2016. Mastering the game of Go with deep neural networks and tree search. *Nature* 529(7587), pp. 484–489, DOI: 10.1038/nature16961.

Singh, V. and Rao, S. 2006. Application of image processing in mineral industry: a case study of ferruginous manganese ores. *Mineral Processing and Extractive Metallurgy Review* 115, pp. 155–160, DOI: 10.1179/174328506X109130.

Song et al. 2017 – Song, L., Liu, S., Yu, M., Mao, Y. and Wu, L. 2017. A Classification Method Based on the Combination of Visible, Near-Infrared and Thermal Infrared Spectrum for Coal and Gangue Distinguishment. *Spectroscopy and Spectral Analysis* 37(02), pp. 416–422, DOI: 10.3964/j.issn.1000-0593(2017)02-0416-07.

Sun et al. 2019 – Sun, Z., Lu, W., Xuan, P., Li, H., Zhang, S., Niu, S. and Jia, R. 2019. Separation of gangue from coal based on supplementary texture by morphology. *International Journal of Coal Preparation and Utilization*, pp. 1–17, DOI: 10.1080/19392699.2019.1590346.

Von Ketelhodt, L. and Carl, B. 2010. Dual energy X-ray transmission sorting of coal. *Journal of the southern African Institute of Mining and Metallurgy* 110(7), pp. 371–378.

Wang, R. 2021. Research on Coal and Gangue Smart Sorting System Base on X-Ray and Structured Light Camera. North University of China (*in Chinese*).

Wang et al. 1998 – Wang, T., Xiao, Y., Yang, Y. and Chase, H. 1998. Fourier transform surface-enhanced Raman spectra of fulvic acid from weathered coal adsorbed on gold electrodes. *Journal of Environmental Science and Health:* Part A 34(3), pp. 749–765, DOI: 10.1080/00387019608007136.

Wang et al. 2021 – Wang, X., Wang, S., Guo, Y., Hu, K. and Wang, W. 2021. Dielectric and geometric feature extraction and recognition method of coal and gangue based on VMD-SVM. *Powder Technology* 392, pp. 241–250.

Xu et al. 2020 – Xu, Z., Lv, Z., Wang, W., Zhang, K. and Lv, H. 2020. Machine vision recognition method and optimization for intelligent separation of coal and gangue. *Journal of China Coal Society* 45(06), pp. 2207–2216 (*in Chinese*).

Xin et al. 2014 – Xin, H., Wang, D., Dou, G., Qi, X., Xu, T. and Qi, G. 2014. The infrared characterization and mechanism of oxygen adsorption in coal. *Spectroscopy Letters* 47(9), pp. 664–675, DOI: 10.1080/00387010.2013.833940.

Xiang et al. 2016 – Xiang, J., Zeng, F., Liang, H., Li, M., Song, X. and Zhao, Y. 2016. Carbon structure characteristics and evolution mechanism of different rank coals. *Journal of China Coal Society* 41(6), pp. 1498–1506, DOI: 10.3390/min8020049.

Zhang et al. 2020 – Zhang, Z., Liu, Y., Hu, Q., Zhang, Z., Wang, L., Liu, X. and Xia, X. 2020. Multi-information online detection of coal quality based on machine vision. *Powder Technology* 374, pp. 250–262, DOI: 10.1016/j.powtec.2020.07.040.

Zhang et al. 2022 – Zhang, J., Han, X. and Cheng, D. 2022. Improving coal/gangue recognition efficiency based on liquid intervention with infrared imager at low emissivity. *Measurement* 189.

Zhu et al. 1987 – Zhu, X., Birringer, R., Herr, U. and Gleiter, H. 1987. X-ray diffraction studies of the structure of nanometer-sized crystalline materials. *Physical Review B* 35(17), pp. 9085–9090.

THE IDENTIFICATION OF COAL AND GANGUE AND THE PREDICTION OF THE DEGREE OF COAL METAMORPHISM BASED ON THE EDXRD PRINCIPLE AND THE PSO-SVM MODEL

Keywords

coal and gangue identification, X-ray diffraction, energy dispersive,
metamorphism degree, PSO-SVM

Abstract

In order to improve the utilization rate of coal resources, it is necessary to classify coal and gangue, but the classification of coal is particularly important. Nevertheless, the current coal and gangue sort-

ing technology mainly focus on the identification of coal and gangue, and no in-depth research has been carried out on the identification of coal species. Accordingly, in order to preliminary screen coal types, this paper proposed a method to predict the coal metamorphic degree while identifying coal and gangue based on Energy Dispersive X-Ray Diffraction (EDXRD) principle with 1/3 coking coal, gas coal, and gangue from Huainan mine, China as the research object. Differences in the phase composition of 1/3 coking coal, gas coal, and gangue were analyzed by combining the EDXRD patterns with the Angle Dispersive X-Ray Diffraction (ADXRD) patterns. The calculation method for characterizing the metamorphism degree of coal by EDXRD patterns was investigated, and then a PSO-SVM model for the classification of coal and gangue and the prediction of coal metamorphism degree was developed. Based on the results, it is shown that by embedding the calculation method of coal metamorphism degree into the coal and gangue identification model, the PSO-SVM model can identify coal and gangue and also output the metamorphism degree of coal, which in turn achieves the purpose of preliminary screening of coal types. As such, the method provides a new way of thinking and theoretical reference for coal and gangue identification.

IDENTYFIKACJA WĘGLA I SKAŁY PŁONNEJ ORAZ PROGNOZOWANIE STOPNIA METAMORFIZMU WĘGLA W OPARCIU O ZASADĘ EDXRD I MODEL PSO-SVM

Słowa kluczowe

identyfikacja węgla i skały płonnej, dyfrakcja rentgenowska, dyspersja energii, stopień metamorfizmu, PSO-SVM

Streszczenie

W celu poprawy stopnia wykorzystania zasobów węgla konieczna jest klasyfikacja węgla i skały płonnej, ale to klasyfikacja węgla jest szczególnie ważna. Niemniej jednak obecna technologia separacji węgla i skały płonnej koncentruje się głównie na identyfikacji węgla i skały płonnej, ale nie przeprowadzono dogłębnych badań dotyczących identyfikacji gatunków węgla. W związku z tym, w celu wstępnego przesiewu rodzajów węgla, w niniejszym artykule zaproponowano metodę przewidywania stopnia metamorfizmu węgla przy identyfikacji węgla i skały płonnej w oparciu o zasadę dyfrakcji rentgenowskiej z dyspersją energii (EDXRD) z 1/3 węglem koksującym, węglem gazowym i skałą płonną z kopalni Huainan w Chinach jako obiektem badawczym. Różnice w składzie fazowym 1/3 węgla koksowego, węgla gazowego i skały płonnej analizowano przez połączenie wzorców EDXRD z wzorcami dyfrakcji rentgenowskiej z dyspersją kątową (ADXRD). Zbadano metodę obliczeniową charakteryzującą stopień metamorfizmu węgla za pomocą wzorców EDXRD, a następnie opracowano model PSO-SVM do klasyfikacji węgla i skały płonnej oraz przewidywania stopnia metamorfizmu węgla. Na podstawie uzyskanych wyników wykazano, że poprzez wbudowanie metody obliczania stopnia metamorfizmu węgla w model identyfikacji węgla i skały płonnej, model PSO-SVM może identyfikować węgiel i skałę płonną, a także wyprowadzać stopień metamorfizmu węgla, co z kolei spełnia cel wstępnego przesiewania rodzajów węgla. Jako taka, metoda ta zapewnia nowy sposób myślenia i teoretyczne odniesienie do identyfikacji węgla i skał płonnych.